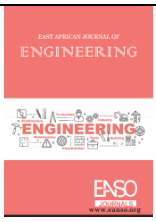

East African Journal of Engineering
eaje.eanso.org
Volume 8, Issue 1, 2025
Print ISSN: 2707-5389 | Online ISSN: 2707-5397
Title DOI: https://doi.org/10.37284/2707-5397

EAST AFRICAN NATURE & SCIENCE ORGANIZATION

Original Article

A Conformal Transformation Technique for Mapping an Open Channel Fluid Flow into a Two-Dimensional Plane

Dr. John Wahome Ndiritu, PhD[1]

[1] Laikipia University, P. O. Box 1100-20300, Nyahururu, Kenya.
[*] Author for Correspondence ORCID ID; https://orcid.org/0000-0002-0119-4017; Email: jwahomestead@gmail.com

Article DOI : https://doi.org/10.37284/eaje.8.1.2687

Publication Date:

10 February 2025

Keywords:

Conformal Mapping, Isogonal Transformation, Free Surface Flow, Direct Method, Indirect Method, Schwarz-Christoffel Theorem.

ABSTRACT

Due to the emergence of many applications in areas of open-channel fluid flow, interest in this branch of fluid mechanics has increased considerably. These areas are wide-ranging, including electricity generation using tidal waves, control of floods and improvement of irrigation systems. Finance, thermal imaging, harnessing of melting of glaciers, flow of fluids over ramps and sluice gates, and quite notably, petroleum exploration are other areas where open channel flow mathematics find great relevance. Whether the free surface of the open channel is being predicted using known bottom characteristics (which is called the 'direct approach'), or the bottom is being inferred from an observable surface (referred to as the 'inverse approach'), researchers often find the need to make computations easier by transforming complex topologies into simpler, more relatable physical equivalents. In this paper, the channel flow of a gravity-influenced Newtonian fluid is treated as the physical w −plane. The fluid is flowing in the positive X direction. The upper half-plane is conformally equivalent to the interior domain determined by any polygon, and the interior points of the physical plane are transformed to the corresponding points above the real axis of the upper half-plane which is then mapped onto the auxiliary half-plane, (the $\wp$ − plane) by being treated as an infinite strip by use of the Schwarz-Christoffel theorem. Assumptions are made that the fluid has dimensional quantities such as uniform speed U_∞ far upstream, and velocity potential Φ. Far upstream before the arbitrary obstacle is encountered, the fluid has a uniform height, h. Then U_∞ and h are used to nondimensionalize the variables to enable computation in a completely non-dimensional environment. With the fluid assumed as steady, inviscid, irrotational and incompressible, w representing the physical w-plane, ξ_i (and t) being points on the auxiliary the $\wp$- plane, θ the angle made by a tangent to this plane at designated points, the required mapping is found to be $\frac{dw}{d\wp} = \frac{k}{\wp}\exp\left[-\frac{1}{\pi}\int_{-\infty}^{\infty}\frac{\theta(t)}{\xi-t}\,dt + \theta(\xi)\right]$.

APA CITATION

Ndiritu, J. W. (2025). A Conformal Transformation Technique for Mapping an Open Channel Fluid Flow into a Two-Dimensional Plane. *East African Journal of Engineering*, *8*(1), 74-85. https://doi.org/10.37284/eaje.8.1.2687

CHICAGO CITATION

Ndiritu, John Wahome. 2025. "A Conformal Transformation Technique for Mapping an Open Channel Fluid Flow into a Two-Dimensional Plane". *East African Journal of Engineering* 8 (1), 74-85. https://doi.org/10.37284/eaje.8.1.2687.

HARVARD CITATION

Ndiritu, J. W. (2025) “A Conformal Transformation Technique for Mapping an Open Channel Fluid Flow into a Two-Dimensional Plane”, *East African Journal of Engineering*, 8(1), pp. 74-85. doi: 10.37284/eaje.8.1.2687.

IEEE CITATION

J. W., Ndiritu “A Conformal Transformation Technique for Mapping an Open Channel Fluid Flow into a Two-Dimensional Plane” *EAJE*, vol. 8, no. 1, pp 74-85, Feb. 2025.

MLA CITATION

Ndiritu, John Wahome. “A Conformal Transformation Technique for Mapping an Open Channel Fluid Flow into a Two-Dimensional Plane” *East African Journal of Engineering*, Vol. 8, no. 1, Feb. 2025, pp. 74-85, doi:10.37284/eaje.8.1.2687.

INTRODUCTION

The complex number $\wp = \xi(x, y) + i\eta(x, y)$ can be represented easily using an Argand diagram by plotting ξ, η and $\wp$ in the same complex space. Any function $f(\wp) = w = x + iy$ will generally be complex, and like $\wp$, a function of x and y. If a point P on the $\wp$-plane is transformed to a corresponding point P' in the w-plane, this process is called the *mapping* of P onto P' under the transformation $w = f(\wp)$, while P' is called the image of P.

Conform and Isogonal Transformations

If the transformations $F(x, y)$ and $\Omega(x, y)$ map two curves C_1 and $C_2$of the $\wp$-plane onto two curves C_1' and C_2' of the w plane respectively and the angle between C_1 and C_2 at the point $\wp = \wp_0$ is equal to the angle between C_1' and C_2' at $\wp = \wp_0$, this transformation is called an *isogonal* transformation. If both the direction of rotation and magnitude of the angle are preserved, the transformation is said to be *conformal*. Therefore, the conditions that a transformation $w = f(\wp)$ be conformal are:

1. $w = f(\wp)$ Should be a regular function of $\wp$ with no singularities, single-valued, have a continuous derivative at every point in the region, and satisfy the Cauchy-Riemann equations.

2. The derivative $\frac{dw}{d\wp}$ Must not vanish, i.e., the transformation must not fail at a critical point.

Common transformations include translation $w = \wp + c$, magnification and rotation, $w = c\,\wp$, and inversion($w = \frac{1}{\wp}$ and $\wp = \frac{1}{w}$), c being a real or complex constant.

Illustrative Examples of Conformal Mapping

In the following adaptations from Ablowitz, & Fokas (2021), John, & Russell (2012), Banjai (2000), and Dennis (2022), conformal mapping is illustrated further by discussing a couple of transformations. The function $w(z) = z + \frac{4}{z}$ is considered, with $f(\wp)$ such that $|\wp| = 1$, (a unit circle).

For $(z) = z + \frac{4}{z}$, a singularity is noted at $z = 0$, and, since $f'(z) = 1 - \frac{4}{z^2}$, critical points at $z = \pm 2$ as well. The transformation is therefore not conformal at the points $(0, +2, -2)$. For the unit circle $|\wp| = 1$, setting $\wp = \xi + i\eta$, it follows that $|\wp| = \eta^2 + \xi^2 = 1$. Additionally, $w = x + iy = z + \frac{4}{z} \quad \Rightarrow \; x + iy = \xi + i\eta + \frac{4}{\xi + i\eta} = \xi + i\eta + \frac{4(\xi - i\eta)}{\xi^2 + \eta^2}$. Equating the real and the complex parts, $x = \xi + \frac{4\xi}{\xi^2 + \eta^2}$ and $y = \eta - \frac{4\eta}{\xi^2 + \eta^2}$. Therefore, $x = 5\xi$ and $y = -3\eta$. (This is because $|\wp| = \eta^2 + \xi^2 = 1$ for the unit circle above). Thus $\xi = \frac{x}{5}$ and $\eta = -\frac{y}{3}$.

The circle $\xi^2 + \eta^2 = 1$ in the $\wp$-plane is mapped to the image $\frac{x^2}{5^2} + \frac{y^2}{3^2} = 1$ in the physical w-plane, which is, in fact, an ellipse with a centre at the origin, major diagonal size 5, and minor diagonal size 3.

In a similar way, the non-linear function $f(\wp) = \wp^2$ which has no singularities and only has a critical point at the origin $\wp = 0$ (because $f'(\wp) = 2\wp = 0$, at $\wp = 0$) may be rendered in exponential form to have $f'(\wp) = \left(re^{i\theta}\right)^2 = r^2 e^{i\,2\theta}$. This clearly shows that the function f doubles the argument and squares the modulus, r. As a result, under $f(\wp) = \wp^2$, the line (complex number)

Article DOI: https://doi.org/10.37284/eaje.8.1.2687

OB in Figure 1 and the annulus $WXYZ$ in Figure 2 are transformed as illustrated.

Figure 1: The Conformal Mapping of a Simple Complex Number under $\boldsymbol{f}(\wp) = \wp^{\mathbf{2}}$

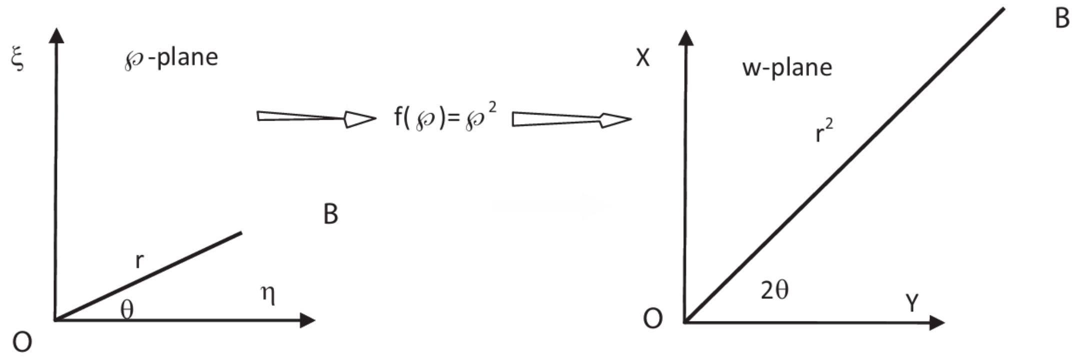

Figure 2: The Conformal Mapping of an Annulus Under $\boldsymbol{f}(\wp) = \wp^{\mathbf{2}}$

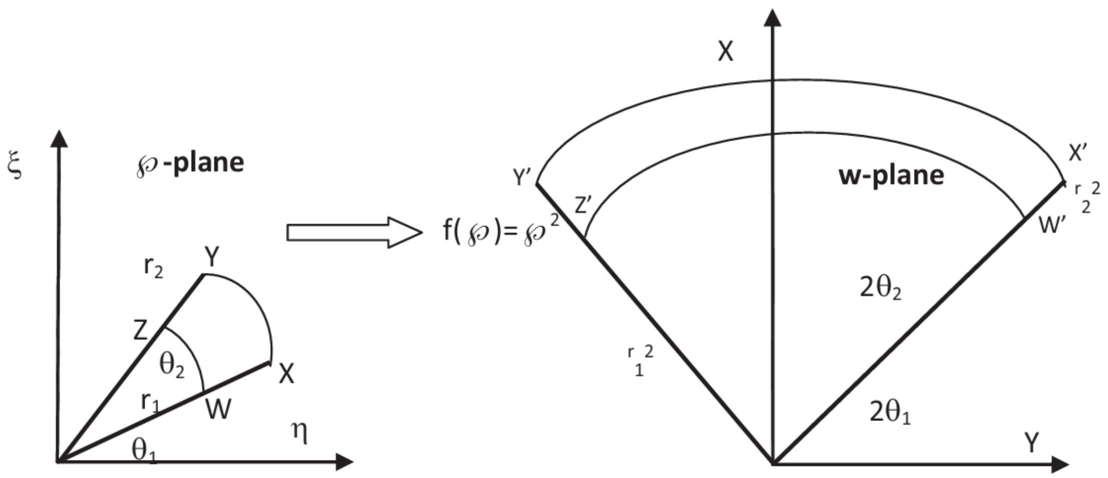

Notably, the angles at the corners W, X, Y and Z, which are in fact right angles, are retained under the transformation, satisfying a key criterion for a conformal mapping.

THE SCHWARZ-CHRISTOFFEL TRANSFORMATION

The Schwarz-Christoffel transformation is a common conformal transformation for mapping the interior of a complicated n-sided physical plane into the upper half of an auxiliary plane that is easier to deal with. Discovered independently in the 1860s by German mathematicians, Elwin Bruno Christoffel and Herman Amandus Schwarz, its accuracy is guaranteed by the Riemann Mapping Theorem that states that any two simply-connected domains with more than one boundary point can be mapped conformally upon one another. This means that the upper half-plane is conformally equivalent to the interior domain determined by any polygon. It is adaptable to solving two-dimensional potential fluid flow problems whereby interior points of the physical plane are transformed to the corresponding points above the real axis of the upper half-plane. More discussion of the foundations of this theorem and its applications are found in Driscoll, & Trefethen (2002), Gonzalo et al. (2008) and Bergonio (2008).

Article DOI: https://doi.org/10.37284/eaje.8.1.2687

Thus, under the Schwarz-Christoffel mapping, any polygon in the physical w-the plane may be made to map onto the entire half of the auxiliary $\wp$ plane, while the boundary of the polygon maps onto the real axis of the $\wp$-plane.

Statement and Proof of the Schwarz-Christoffel Theorem

> ***Theorem 1*** [Schwarz-Christoffel]. *Let P be a simple, closed polygon with n vertices. Let $w_1, w_2 \dots, w_n$ be points coinciding with the apexes of a polygon in the w-plane (physical plane) and which are mapped onto the points*
>
> $\xi_1 < \xi_2 < \cdots < \xi_n$
>
> *In the real axis of the $\wp$ (auxiliary) plane. Let the polygon have interior angles α_k, where $\alpha_1 + \alpha_2 + \cdots + \alpha_n = (n-2)\pi$ which are positioned at the corners of the polygon designated by the points $w_1, w_2 \dots, w_n$ above. The transformation from the $\wp$-plane to the w-plane is defined in terms of the derivative $f'(\wp)$ as*

$$w = K_0 \int \left\{\left[(\wp - \xi_1)^{\frac{\alpha_1}{\pi}-1}(\wp - \xi_2)^{\frac{\alpha_2}{\pi}-1} \dots (\wp - \xi_n)^{\frac{\alpha_n}{\pi}-1}\right\}\right] d\,\wp + K_1 \qquad (1)$$

with K_0 and K_1 being suitably chosen constants.

In differential form, equation (1) is,

$$\frac{dw}{d\wp} = K_0(\wp - \xi_1)^{\frac{\alpha_1}{\pi}-1}(\wp - \xi_2)^{\frac{\alpha_2}{\pi}-1}(\wp - \xi_3)^{\frac{\alpha_3}{\pi}-1} \dots \qquad (2)$$

Here, K_0 is a constant which may be complex. Thus, the Schwarz-Christoffel theorem transforms the real axis of the $\wp$-plane into the boundary of the polygon P in the w-plane such that the vertices of the polygon at which the interior angles are the $\alpha_1, \alpha_2 \dots \alpha_n$ corresponds to the points $w_1 < w_2 < \cdots < w_n$. When the polygon is simple, the interior is mapped by the transformation onto the upper plane of the $\wp$-plane. This setting, elaborated well in Floryan et al. (1987) is illustrated below in Figure 3.

Figure 3: Illustrative Diagram for Schwarz-Christoffel Transformation with n = 5

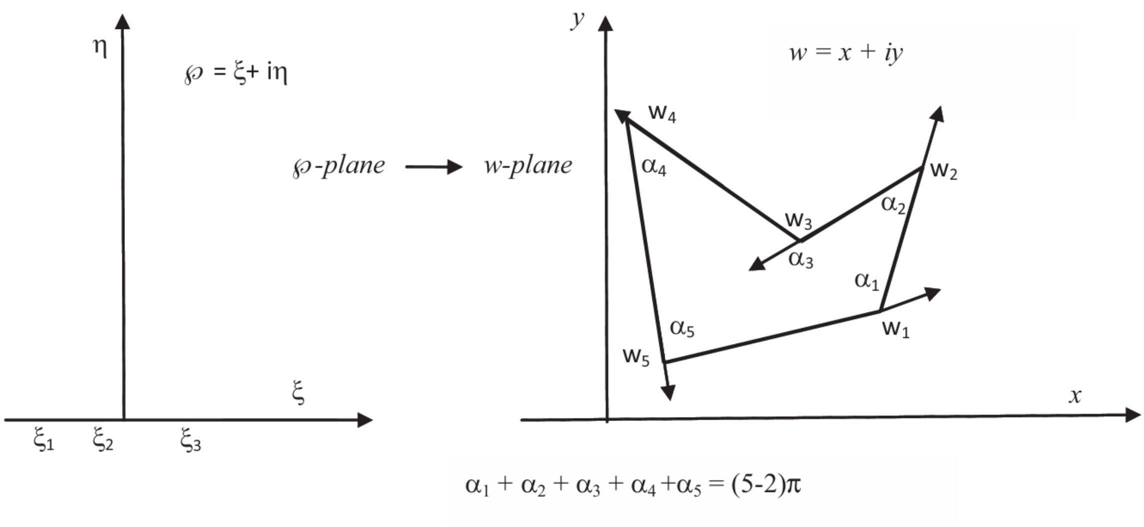

Proof of the Schwarz-Christoffel Theorem

A detailed derivation of the Schwarz-Christoffel transformation and a wide account of its varied application is provided in the classic book by Milne-Thompson (1957). Comprehensive proofs are available in Driscoll, & Trefethen (2002) Brown, & Churchill (2009), among other sources.

An informal justification for the transformation, however, is provided as follows. Given equation (2), consider a family of infinitesimal increments $d\wp$ along the real axis in the $\wp$ plane, and their images dw in the w plane. This is done by exploring the arguments $arg(d\wp)$, of the increments $d\wp$. Equation (2) is equivalent to

Article DOI: https://doi.org/10.37284/eaje.8.1.2687

$$\arg(dw) = \arg(d\wp) + \arg(K_0) + \left(\frac{\alpha_1}{\pi} - 1\right)\arg(\wp - \xi_1) + \left(\frac{\alpha_2}{\pi} - 1\right)\arg(\wp - \xi_2) + \left(\frac{\alpha_3}{\pi} - 1\right)\arg(\wp - \xi_3) \ldots + \left(\frac{\alpha_n}{\pi} - 1\right)\arg(\wp - \xi_n) \quad (3)$$

Along the real axis in the positive direction, a time comes when $\wp$ is between consecutive ξ_i. At that instance, every term of the equation (3) is constant. The implication is that w moves in a straight line. This explains why the image of w-plane is polygonal. To investigate the behaviour at the singular points (corners), it is noted that when $\wp = \xi_i$ not only do all the terms in the equation (3) other than the ones containing the ξ_i have a constant value as mentioned already, but $arg(\wp - \xi_i)$ jumps from the value π when $\wp < \xi_i$ to a value 0 for values greater than ξ_i. This also implies that the value of $\left(\frac{\alpha_i}{\pi} - 1\right)\arg(\wp - \xi_i)$ jumps from $\alpha_i - \pi$ to the value 0. The direction of traversal of w has an anti-clockwise rotation (positive) by a magnitude of $(\pi - \alpha_i)$, necessitating the introduction of an angle α_i newly in the polygon. The mapping is one-to-one and maps the upper half plane to the interior of a polygon. Driscoll, & Trefethen (2002) and Wolfram (1999) give more details. Moreover, the real axis maps to the boundary of a polygonal region.

Generalized Schwarz-Christoffel Theorem in Exponential Form

The equation (2) may be written as the product,

$$\frac{dw}{d\wp} = K_0 \prod_{i=1}^{n} (\wp - \xi_i)^{\frac{\alpha_i}{\pi} - 1} \quad (4)$$

Taking the logarithm, and bearing in mind that

$$\log \wp = \log \quad |\wp| + i \arg(\wp) \quad (5)$$

then,

$$\log \quad \frac{dw}{d\wp} = \log K_0 + \sum_{i=1}^{n} \left(\frac{\alpha_i}{\pi} - 1\right) \log(\wp - \xi_i) \quad (6)$$

and

$$\log\left(\frac{dw}{d\wp}\right) + i \arg \quad \left(\frac{dw}{d\wp}\right) = \log|K_0| + i \arg K_0 + \sum_{i=1}^{n} \left(\frac{\alpha_i}{\pi} - 1\right) [\log|\wp - \xi_i| + i \arg(\wp - \xi_i)] \quad (7)$$

Equating the real and imaginary parts of the equation (7) it is noted that

$$\arg\left(\frac{dw}{d\wp}\right) = \arg K_0 + \sum_{i=1}^{n} \left(\frac{\alpha_i}{\pi} - 1\right) \arg(\wp - \xi_i) \quad (8)$$

and

$$\arg(dw) = \arg(d\wp) + \arg K_0 + \sum_{i=1}^{n} \left(\frac{\alpha_i}{\pi} - 1\right) \arg(\wp - \xi_i) \quad (9)$$

which is the unexpanded form of equation (3).

Figure 4 below, represents the i^{th} segment in the physical w −plane, with θ_i being the angle made by the tangent to a smooth curve in this plane at the point which corresponds to the real axis in the $\wp$ − plane.

Figure 4: The i^{th} Angles of the Physical w-plane

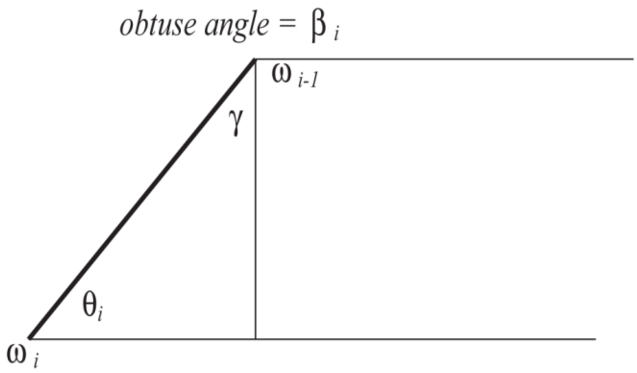

Article DOI: https://doi.org/10.37284/eaje.8.1.2687

Clearly,

$$\beta_i + \left(\frac{\pi}{2} - \theta_i\right) + \frac{\pi}{2} = 2 \qquad (10)$$

$$\beta_i = \pi + \theta_i \qquad and \qquad \beta_{i+1} = \pi + \theta_{i+1} \qquad (11)$$

For some $\epsilon < \xi_i$, that is $\epsilon - \xi_i < 0$, there exists a term $\arg(\epsilon - \xi_i) = \pi$ emanating from equation (8). For the $(i+1)^{th}$segment, it follows that, $\epsilon - \xi_i > 0$, which means that, $\wp$ is now on the positive real axis and $\arg(\epsilon - \xi_i) = 0$. Therefore, the angle subtended by the i^{th} segment is

$$\beta_{(i+1)} = \beta_i - \left(\frac{\alpha_i}{\pi} - 1\right) \qquad (12)$$

Invoking the equations (9) and (11) the result is,

$$\pi + \theta_{(i+1)} = \pi + \theta_i - \left(\frac{\alpha_i}{\pi} - 1\right)\pi, \ \theta_{i+1} - \theta_i = \pi\left(\frac{\alpha_i}{\pi} - 1\right) \qquad (13)$$

Applying the Mean Value Theorem (MVT), whose general form is

$$f(x_{i+1}) - f(x_i) = f'(\tilde{x})(x_{i+1} - x_i) \qquad (14)$$

where $\tilde{x}$ lies between x_{i+1} and x_i.

In terms of θ, the MVT is equivalent to

$$\theta_{(i+1)} - \theta_i = (\xi_{i+1} - \xi_i)\,\theta'(\tilde{\xi_i}) \qquad (15)$$

Where $\theta_i = \theta(\xi_i)$. Applying the equation (15) in (8) and additionally letting $n \to \infty$ and $\xi_{(i+1)} - \xi_i \to 0$, it is noted that

$$\log\left(\frac{dw}{d\wp}\right) = \log K_0 + \sum_{i=1}^{n}\left(\frac{-1}{\pi}\right)(\xi_{i+1} - \xi_i)\theta'(\xi_i)\log(\wp - \xi_i) \qquad (16)$$

Replacing the finite term with an integral,

$$\log\left(\frac{dw}{d\wp}\right) = \log K_0 - \frac{1}{\pi}\int_a^b \theta'(\xi)\log(\wp - \xi)\,d\xi \qquad (17)$$

The generalized Schwarz-Christoffel form in exponential form has been obtained, which is

$$\frac{dw}{d\wp} = K_0 \exp\left[\frac{-1}{\pi}\int_a^b \theta'(\xi)\log(\wp - \xi)\ d\xi\right] \qquad (18)$$

θ in the above discussion represents the angle made by the tangent to a smooth curve in the w −plane to the point corresponding to the real axis in the $\wp$-plane.

APPLICATION OF THE SCHWARZ-CHRISTOFFEL THEOREM TO MAP AN INFINITE STRIP

Considering an infinite strip Q_∞, R_∞, R'_∞, Q'_∞ which has a height h in the physical,$w-$plane. Let the physical setting be as in the Figure (5). Letting it open out, and the points R'_∞, $and\ Q'_\infty$ to coincide, all the points in the $w-$plane boundaries are therefore mapped onto the real axis of the $\wp$-plane. The points R'_∞, $and\ Q'_\infty$ are placed at $\wp = 0$ that is, at the origin of the $\wp$-plane. Let the points $H(0,h)$ and $O(0,0)$ in the physical $w-$plane map to the points $\xi = +1$ and $\xi = -1$, in the $\wp$-plane.

Figure 5 shows that Q_∞ and Q'_∞on the physical plane are mapped respectively onto $\xi = -\infty$ and $\xi = \infty$ in the $\wp$ −plane. Since the points R_∞ and R'_∞in the physical plane are infinitely far from the origin and the argument of R'_∞ is tending to zero, the conclusion is that these two points are coincident and make an angle of zero between them.

Article DOI: https://doi.org/10.37284/eaje.8.1.2687

Figure 5: The Physical Plane (w-plane)

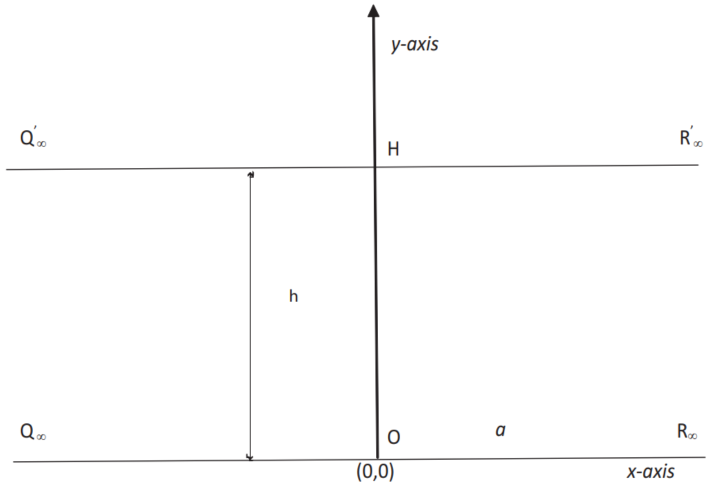

Figure 6: The Upper Half-plane(℘-plane)

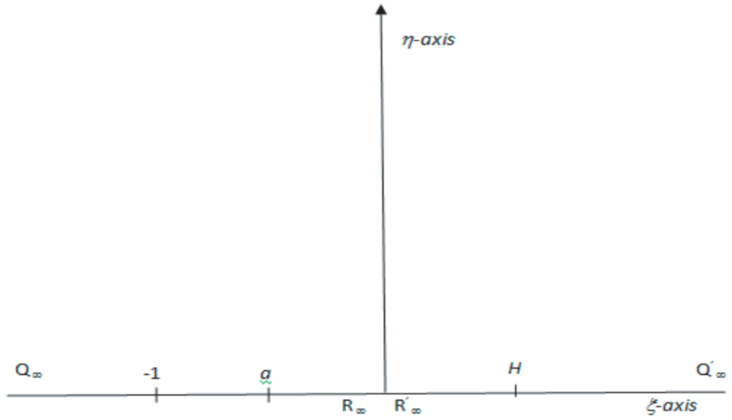

The Schwarz-Christoffel theorem is used to transform this infinite strip in the physical plane into the upper half-plane. Given equation (2) and the information just above, that is, the angle between R_∞ and R'_∞ is vanishing, and the coincident point is $\xi = 0$, then,

$$\frac{dw}{d\wp} = K_0(\wp)^{-1} \qquad (19)$$

thus,

$$w = K_0 ln(\wp) + K_1 \qquad (20)$$

With determinable constants K_0 and $K_1 \in \Re$, or are complex.

Since the mapping as described above satisfies $w(\wp): -1 \mapsto 0$ substituting those values into equation (20).

$$0 = K_0\, ln(-1) + K_1 \ (21)$$

$w(\wp): 1 \mapsto ih$ values which are inserted into the equation (21) to obtain

$$ih = K_0\, ln(1) + K_1 \qquad (22)$$

Since of the fact that $\ln 1 = 0$ the equation (22)

$$K_1 = ih (23)$$

is obtained. Moreover,

$$0 = K_0 ln(-1) + K_1 = K_0 \ln(-1) + ih \quad (24)$$

which implies that

$$K_0 \ln(-1) = -ih \qquad (25)$$

that is,

$$K_0 = \frac{-ih}{\ln(-1)} = \frac{-ih}{\ln i^2} = \frac{-ih}{2\ln i} \qquad (26)$$

Since

Article DOI: https://doi.org/10.37284/eaje.8.1.2687

$e^{\frac{\pi}{2}} = \cos\frac{\pi}{2} + i\sin\ \ \frac{\pi}{2} = i$ (27)

It follows that

$\ln i = \frac{\pi}{2}$(28)

Equation (60) becomes

$K_0 = \frac{-ih(2)}{2\pi(i)} = \frac{-h}{\pi}$ (29)

This makes the equation (60) to finally become,

$w = \frac{-h}{\pi}\ln(\wp) + ih$ (30)

which is equivalent to

$\ln(\wp) = i\pi - \frac{\pi}{h}w$ (31)

To obtain the requisite conformal mapping that transforms all the points in the real axis of $\wp -$ plane into the points in the interior of the w −plane, the inverse logarithm of the equation (31) is taken and the equation (32) below is obtained.

$\wp = -e^{-\frac{\pi}{h}w}$ (32)

SCHWARZ-CHRISTOFFEL TRANSFORMATION APPLIED TO CHANNEL FLOW PROBLEM

Physical Setting of the Problem

The channel flow of a gravity-influenced Newtonian fluid is treated as the physical w −plane. The fluid is flowing in the positive X direction. This plane is then mapped onto the auxiliary half-plane, that is the $\wp -$ plane in a way similar to the mapping of the infinite strip, by use of the Schwarz-Christoffel theorem. The assumptions are made that the fluid has dimensional quantities such as uniform speed U_∞ far upstream, and velocity potential Φ. Far upstream before the arbitrary obstacle is encountered, the fluid has a uniform height, h. Then U_∞ and h are used to nondimensionalize variables to enable us to work in a completely non-dimensional environment. After the non-dimensionalization of the problem in the section below, the setting becomes as illustrated in the figure (8).

Figure 8: Channel Flow Problem with Dimensionless Variables, to which the Schwarz-Christoffel Transformation is Applied.

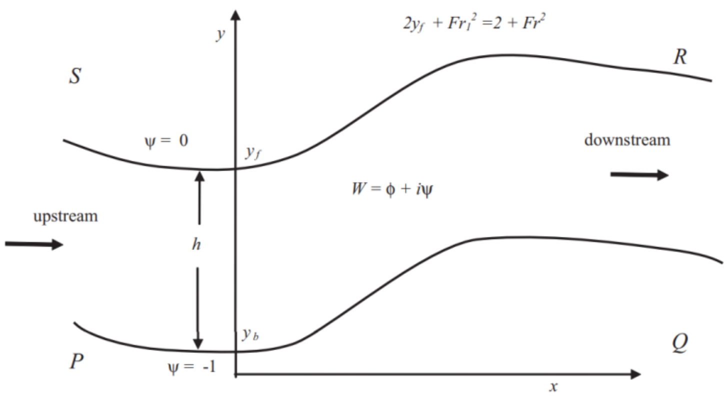

Non-dimensionalization of the Problem

The attraction between microscopic particles of the flowing liquid and those of the boundary material gives rise to surface tension forces. In the two-dimensional type of flow being considered in this study (which is also steady, inviscid, irrotational, and incompressible, as already mentioned), the consequence of the surface tension force is a disparity in the surface pressure.

If P_0, P_1, γ and R respectively represent the dimensional fluid pressures at either side of the free boundary, surface tension and radius of curvature of the surface, at the free surface $Y = Y_f(x)$ that,

$P_1 - P_0 = \frac{\gamma}{R}$ (33)

Article DOI: https://doi.org/10.37284/eaje.8.1.2687

Suppose $\check{S}$is the dimensional arclength and θ the angle made by the free surface with the horizontal and using the approach found in Acheson (1990), then,

$$R\delta\theta = \delta\check{S} \Rightarrow R = \frac{d\check{S}}{d\theta} \quad (34)$$

So that equation (33) becomes

$$P_1 - P_0 = \frac{\gamma}{\frac{d\check{S}}{d\theta}} \quad (35)$$

The free boundary condition for this type of flow is provided by the Bernoulli equation as

$$\frac{P_1 - P_0}{\rho g h} + \frac{Y_f}{h} + \frac{U_f^2}{2gh} = 1 + \frac{U_\infty^2}{2gh} \quad (36)$$

Here, h and U_∞ represents the upstream *dimensional* depth and velocity respectively, Y_f and U_f the fluid height and *dimensional* fluid velocity on the surface, respectively. Invoking the last two immediate equations (35) and (36) then,

$$\frac{\gamma}{\rho g h \frac{d\check{S}}{d\theta}} + \frac{Y_f}{h} + \frac{U_f^2}{2gh} = 1 + \frac{U_\infty^2}{2gh} \quad (37)$$

which is the same as

$$\frac{U_f}{U_\infty} = \sqrt{\left\{\left[1 + 2\frac{\left(1-\frac{Y_f}{h}\right)}{F_r^2} + 2\,h\,We\left(\frac{d\theta}{d\check{S}}\right\}\right)\right]} \quad (38)$$

with $F_r = \frac{U_\infty}{\sqrt{gh}}$ and $\mathrm{We} = \frac{\gamma}{\rho g (hF_r)^2}$ the Weber number. Much like the Mach number, the Froude number is a *non-dimensional* parameter that plays a crucial role in describing the behaviour of a fluid in open channel flow as elucidated in greater detail by Munson et al. (1994), Gerhart et al. (2020), and Lonyangapuo (1999).

The Weber number, We is a *dimensional* parameter $We = \frac{inertia\ force}{surface\ tension\ force}$. Neglecting the surface tension and viscous forces, the Bernoulli equation becomes

$$\frac{Y_f}{h} + \frac{U_f^2}{2gh} = 1 + \frac{U_\infty^2}{2gh} \quad (39)$$

No fluid penetrates the bottom, and no fluid leaves the flow.

The summary of the important *non-dimensional* quantities follows.

$$x = \frac{X}{h}, y = \frac{Y}{h}, s = \frac{S}{h}, u = \frac{U}{U_\infty}, v = \frac{V}{U_\infty}, p = \frac{P}{\rho U_\infty^2},$$

$$u_f = \frac{U_f}{U_\infty}, y_f = \frac{Y_f}{h}, \phi = \frac{\Phi}{hU_\infty} \text{ and } \psi = \frac{\Psi}{hU_\infty} \quad (40)$$

The Laplace equation is expressed as

$$\frac{\partial^2\phi}{\partial x^2} + \frac{\partial^2\phi}{\partial y^2} = 0, -\infty < x < \infty, y_b < y < y_f$$

$$\frac{\partial^2\psi}{\partial x^2} + \frac{\partial^2\psi}{\partial y^2} = 0,, -\infty < x < \infty, y_b < y < y_f \quad (41)$$

Also, equations (38) and (39) similarly become

$$u_f = \sqrt{\left[1 + \frac{2(1-y_f)}{F_r^2}\right]} \quad (42)$$

and

$$2y_f + \breve{F_r^2} = 2 + F_r^2 \quad (43)$$

With

$$\breve{F}_r = \frac{U_f^2}{\sqrt{gh}} \text{ and } y_f = \frac{Y_f}{h} (44)$$

(y_f *is* the non-dimensionalized height of the free surface).

The situation at the solid boundary is now considered. Let $\vec{V}$ be the dimensional velocity of the fluid and $\breve{\vec{V}}$ the dimensional velocity of the solid boundary. If $\vec{n}$ is a unit normal vector to the boundary, and since the fluid cannot cross the impermeable wall of the channel, it is expected the velocity of the fluid at the boundary must have its component normal to the boundary equal to the normal component of the velocity at the boundary. Mathematically, that means

$$\vec{V} \cdot \vec{n} = \breve{\vec{V}} \cdot \vec{n} \ (45)$$

EQUATIONS OF TRANSFORMATION

In a transformation similar to that of the infinite strip, the physical plane of Figure (3) is mapped onto the auxiliary upper half plane as follows in Figure (9).

Article DOI: https://doi.org/10.37284/eaje.8.1.2687

Figure 9: Physical Plane After Being Mapped onto the Half-plane Using Schwarz-Christoffel Transformation

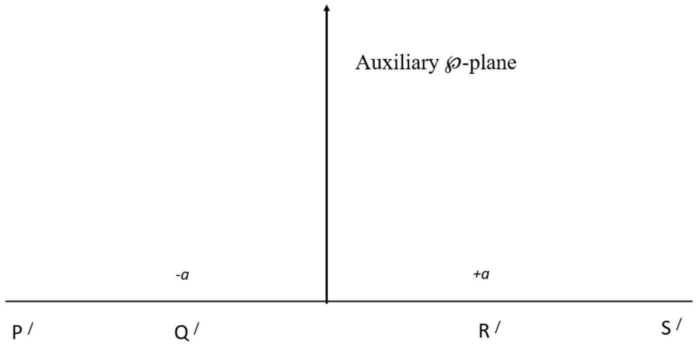

In view of the theorem with the angle $\alpha = 90^0$ Q is mapped onto Q' by the transformation

$$\left(\wp - (-a)\right)^{\frac{\frac{\pi}{2}}{\pi}-1} \qquad (46)$$

which is equivalent to

$$(\wp + a)^{-\frac{1}{2}} \qquad (47)$$

Similarly, R also maps to R' by the transformation

$$(\wp - a)^{-\frac{1}{2}} \qquad (48)$$

This makes the total transformation of $\overline{QR}$ to $\overline{Q'R'}$ therefore become

$$[(\wp + a)(\wp - a)]^{-\frac{1}{2}} \qquad (49)$$

The curved channel bed PQ and bottom RS are transformed by the equation (18) to respectively have

$$\int_{-\infty}^{-a} \theta' \ln(\wp - \xi)\, d\xi = [\theta(\xi)\ln(\wp - \xi)]_{-\infty}^{-a} - \int_{-\infty}^{-a} \frac{\theta(\xi)}{\wp - \xi} \times (-1)\, d\xi \qquad (50)$$

and

$$\int_{a}^{\infty} \theta' \ln(\wp - \xi)\, d\xi = [\theta(\xi)\ln(\wp - \xi)]_{a}^{\infty} + \int_{a}^{\infty} \frac{\theta(\xi)}{\wp - \xi} d\xi \qquad (51)$$

after integration by parts.

But since $\theta(-a), \theta(a), \theta(\infty)$, and $\theta(-\infty)$ all vanish, the terms containing the logarithm in the equations (50) and (51) vanish as well so that,

$$\int_{-\infty}^{-a} \frac{\theta(\xi)}{\wp - \xi}\, d\xi \quad \text{and} \quad \int_{a}^{\infty} \frac{\theta(\xi)}{\wp - \xi} d\xi \qquad (52)$$

Given the equations (18), (49) and (52) and applying elementary rules for indices, the total transformation now becomes

$$\frac{dw}{d\wp} = k[(\wp + a)(\wp - a)\backslash big]^{-\frac{1}{2}} \exp\left[-\frac{1}{\pi}\int_{-\infty}^{-a} \frac{\theta(\xi)}{\wp - \xi} d\xi - \frac{1}{\pi}\int_{a}^{\infty} \frac{\theta(\xi)}{\wp - \xi} d\xi\right] \qquad (53)$$

But quite clearly,

$$\lim_{PQ \to \infty} a = 0 \qquad (54)$$

Taking into account the continuity of the limits of integration, equation (53) may now be written as

$$\frac{dw}{d\wp} = \frac{k}{\wp} \exp\left[-\frac{1}{\pi}\int_{-\infty}^{\infty} \frac{\theta(\xi)}{\wp - \xi}\, d\xi\right] \qquad (55)$$

So far, the symbol ξhas been used to represent increments in the real axis of the ℘-plane. To conserve the nomenclature for the half-plane, ξ is replaced with t in the last equation above so that,

$$\frac{dw}{d\wp} = \frac{k}{\wp} \exp\left[-\frac{1}{\pi}\int_{-\infty}^{\infty} \frac{\theta(t)}{\wp - t}\, dt\right] \qquad (56)$$

In view of the equation (56) alongside the equation for the upper half-plane, $\wp = \xi + i\eta$ the limit, $\lim_{\wp \to \xi + i0^+} \int_{\infty}^{-\infty} \frac{\theta(t)}{\wp - t}\, dt$ is investigated.

Quite clearly,

$$\lim_{\wp \to \xi + i0^+} \int_{-\infty}^{\infty} \frac{\theta(t)}{\wp - t}\, dt = \left[\lim_{\wp \to \xi + i0^+} \int_{-\infty}^{\infty} \frac{\theta(t)(\xi - t)(dt)}{(\xi - t)^2 + \eta^2\, dt} - i \int_{-\infty}^{\infty} \frac{\eta\theta(t)dt}{(\xi - t)^2 + \eta^2}\right] \qquad (57)$$

Article DOI: https://doi.org/10.37284/eaje.8.1.2687

that is after separating the complex and real terms. The limit of the non-complex term in the equation (57) clearly becomes,

$$\int_{\infty}^{-\infty} \frac{\theta(t)}{\xi - t}\, dt \qquad (58)$$

when the complex part of the equation (57) is considered.

Letting $\eta\check{t} = \xi - t \Rightarrow t = \xi - \eta\check{t}, dt = -\eta d\check{t}$, the complex part changes variables to be

$$\lim_{\wp \to \xi + i0^+} \int_{-\infty}^{\infty} \frac{\theta(t)}{\wp - t}\, dt = \left[\lim_{\wp \to \xi + i0^+} \int_{-\infty}^{\infty} \frac{\theta(t)(\eta - t)}{(\xi - t)^2 + \eta^2}\, dt\right\} - \mathrm{i} \int_{\infty}^{-\infty} \frac{\eta\, \theta(t)}{(\xi - t)^2 + \eta^2}\, (\mathrm{dt}) \qquad (59)$$

CONCLUSION

A fluid flow with dimensional quantities and uniform speed U_∞, uniform height h and velocity potential Φ far upstream before the arbitrary obstacle is encountered has been considered. U_∞ and h are used to nondimensionalize the variables to enable computation in a completely non-dimensional environment. The fluid is assumed as steady, inviscid, irrotational and incompressible, with *w* representing the physical *w*-plane, θi the angle made by a tangent to a smooth curve on this plane at designated points.

Then,

$$\int_{-\infty}^{\infty} \frac{\theta(t)}{\wp - t} = \int_{\infty}^{-\infty} \frac{\theta(t)}{\xi - t}\, dt - i\pi\theta(\xi) (60)$$

The required mapping is,

$$\frac{dw}{d\wp} = \frac{k}{\wp} \exp\left[-\frac{1}{\pi} \int_{-\infty}^{\infty} \frac{\theta(t)}{\xi - t}\, dt + \theta(\xi)\right] \qquad (61)$$

FUTURE WORK

One of the assumptions made in this study is that only the flow occurred solely subject to gravitational forces. In practice, surface tensional forces which were neglected have some effects, which, however minimal, will always affect boundary conditions. Research in this field with consideration of surface tension would be very appropriate.

Another natural development of this study would be to extend it from two to three dimensions, which mirrors most closely to reality. As expected, because of the increase in boundary conditions and more sophistication of the equations governing the flow, the computations would be much more complex. However, with the availability of computers with ever-increasing computational power and sophisticated multi-dimensional algorithms, this is attainable.

REFERENCES

Ablowitz, M. J., & Fokas, A. S. (2021). *Introduction to Complex Variables and Applications.* Cambridge: Cambridge University Press.

Acheson, D.J. (1990). *Elementary fluid dynamics.* Clarendon Press, New York.

Banjai, L. (2000). *Recursive algorithms in complex analysis*. Oxford University

Bergonio, P.P. (2008). *Schwarz-Christoffel transformations*. Georgia Southwestern State University.

Brown, J.W., & Churchill, R.V. (2009). *Complex Variables and Applications, 8th Edition.* McGraw Hill Higher Education.

Dennis, G.Z. (2022). *Engineering Mathematics, 7th Edition*. Jones and Bartlett Publishers.

Driscoll T.A., & Trefethen L.N. (2002). *Schwarz-Christoffel Mapping*. Cambridge University Press.

Floryan, J.M., & Zemach, C. (1987). *Schwarz-Christoffel mappings: A General approach.* Journal of Computational Physics 72(2), pp 347-371

Gerhart A.L., Hochstein, J.I., & Gerhart, P. M. (2020). *Fundamentals of Fluid Mechanics, 9th Edition*. John Wiley & Sons.

Gonzalo, R., Hernan, C., & Ruben, P. (2008). *The Schwarz-Christoffel conformal mapping for Polygons with Infinitely Many Sides. International Journal of Mathematics and*

Article DOI: https://doi.org/10.37284/eaje.8.1.2687

Mathematical, Sciences Volume 2008. Hindawi Publishing Corporation.

John, M., & Russell, H. (2012). *Complex analysis for mathematics and engineering, sixth edition.* Jones and Bartlett Publishers.

Lonyangapuo, J.K. (1999). *Bottom surface identification for known free surface fluid flows*. PhD thesis, University of Leeds.

Milne-Thompson, L.M. (1957). *Theoretical Hydrodynamics*. Macmillan, London.

Munson, B. R., Young, D.F., & Okiishi, T.H. (1994). *Fundamentals of fluid mechanics*. John Willey and Sons, New York.

Wolfram, K. (1999). *Schwarz-Christoffel mappings: symbolic computation of mapping functions for symmetric polygonal domains*. Freie Universitat Berlin.